

# Upper Limit on the Branching Ratio for the Decay $\pi^0 \rightarrow \nu\bar{\nu}$

M. S. Atiya, I-H. Chiang, J. S. Frank, J. S. Haggerty, M. M. Ito,<sup>(a)</sup> T. F. Kycia, K. K. Li,  
L. S. Littenberg, A. Stevens, and R. C. Strand  
*Brookhaven National Laboratory, Upton, New York 11973*

W. C. Louis

*Medium Energy Physics Division, Los Alamos National Laboratory, Los Alamos, New Mexico 87545*

D. S. Akerib,<sup>(b)</sup> D. R. Marlow, P. D. Meyers, M. A. Selen,<sup>(b)</sup> F. C. Shoemaker, and A. J. S. Smith  
*Joseph Henry Laboratories, Princeton University, Princeton, New Jersey 08544*

G. Azuelos,<sup>(c)</sup> E. W. Blackmore, D. A. Bryman, L. Felawka, P. Kitching, Y. Kuno, J. A. Macdonald,  
T. Numao, P. Padley, J-M. Poutissou, R. Poutissou, and J. Roy  
*TRIUMF, Vancouver, British Columbia, Canada V6T 2A3*  
(Received 26 December 1990)

An experimental upper limit on the branching ratio for the decay  $\pi^0 \rightarrow \nu\bar{\nu}$  is set at  $8.3 \times 10^{-7}$  (90% C.L.). This decay is forbidden if neutrinos are purely left handed. The limit also applies to any decays of the  $\pi^0$  to weakly interacting neutrals.

PACS numbers: 13.20.Cz, 14.60.Gh

The decay  $\pi^0 \rightarrow \nu\bar{\nu}$  is forbidden by angular momentum conservation if the neutrino has purely left-handed helicity. This is the case in the standard model if the neutrinos are massless. If the neutrino mass is not zero and the  $Z^0$  couples to the right-handed neutrino with standard weak-interaction strength, the branching ratio  $B(\pi^0 \rightarrow \nu\bar{\nu})$  has a maximum value<sup>1</sup> of  $3 \times 10^{-9}$  at  $m_{\nu} = 55 \text{ MeV}/c^2$ . The current upper limit<sup>2</sup>  $m_{\nu} \leq 35 \text{ MeV}/c^2$  implies that  $B(\pi^0 \rightarrow \nu\bar{\nu}) < 2 \times 10^{-9}$ . The minimal Higgs boson of the standard model does not contribute to the decay, but some extensions to the standard model contain additional Higgs bosons that give contributions larger than  $Z^0$  exchange.<sup>3</sup> More exotic are the possibilities of the decay of the  $\pi^0$  into new, undetectable particles,<sup>4</sup> or of violation of lepton-number conservation, which might allow the process  $\pi^0 \rightarrow \nu\nu'$ . In the class of decays  $\pi^0 \rightarrow$  "nothing," where "nothing" is any system of weakly interacting neutrals, there is thus no contribution from pairs of massless neutrinos, as there is in processes such as  $Z^0$  decay and  $e^+e^- \rightarrow \gamma X$ , and there is no Glashow-Iliopoulos-Maiani suppression, as there is in flavor-changing neutral currents. Our investigation thus complements other searches for physics beyond the standard model.

The limit reported here is a result of our search<sup>5</sup> for the rare decay  $K^+ \rightarrow \pi^+\nu\bar{\nu}$ , where detection of the photons from  $\pi^0$  decay is crucial to suppress the background  $K^+ \rightarrow \pi^+\pi^0$ . It is this latter decay that allows us access to a process in which neither the initial nor the final state is observed. Reconstruction of a  $\pi^+$  of momentum 205 MeV/c from a  $K^+$  decay at rest tags the presence of a 205-MeV/c  $\pi^0$  in our detector.

Prior experimental limits on the branching ratio for  $\pi^0 \rightarrow \nu\bar{\nu}$  are of two types. Reanalysis<sup>3</sup> of an older

$K^+ \rightarrow \pi^+\nu\bar{\nu}$  search<sup>6</sup> yields a 90%-C.L. upper limit of  $2.4 \times 10^{-5}$ . An analysis of beam-dump neutrino production<sup>7</sup> yields  $8.3 \times 10^{-6}$ , after a background subtraction. This method requires the final-state particles to be  $\nu_e, \nu_\mu$ , or  $\nu_\tau$ . Astrophysical processes can be used to infer bounds that can be substantially lower, but are very model dependent.<sup>8</sup>

The detector, shown in Fig. 1, is described in Ref. 5. In summary,  $K^+$ 's from the Low Energy Separated Beam (LESB I) at the Brookhaven Alternating Gradient Synchrotron are identified in the Cherenkov counter, lose energy in the degrader, and come to rest in the scintillating-fiber target. Charged decay products are measured in a spectrometer covering  $2\pi$  sr of solid angle and consisting of a cylindrical drift chamber, a scintillator range stack, and a solenoidal magnet. The spectrometer measures momentum, kinetic energy, and range, with resolutions of 2.6%, 2.9%, and 4.2% at the  $K^+ \rightarrow \pi^+\pi^0$  peak. The  $\pi^+$ 's are unambiguously identified by comparing the range and momentum of charged tracks, and through observation of the  $\pi^+ \rightarrow \mu^+ \rightarrow e^+$  decay chain in transient digitizers instrumenting the range-stack counters.

Given the presence of a  $\pi^0$ , the limit presented here is determined entirely by how well we can reject  $\pi^0 \rightarrow \gamma\gamma$  decays. The methods for doing this are effective against  $\pi^0 \rightarrow \gamma e^+e^-$  decays as well. Photons are detected in  $4\pi$  sr of solid angle. Two detectors are specifically designed for this purpose: a 14-radiation-length-thick barrel photon veto surrounding the range stack, and 12-radiation-length-thick end caps at each end of the drift chamber. Both detectors are inside the magnet. They are constructed of alternating layers of 5-mm scintillator and 1-mm lead. The fine segmentation of the other de-

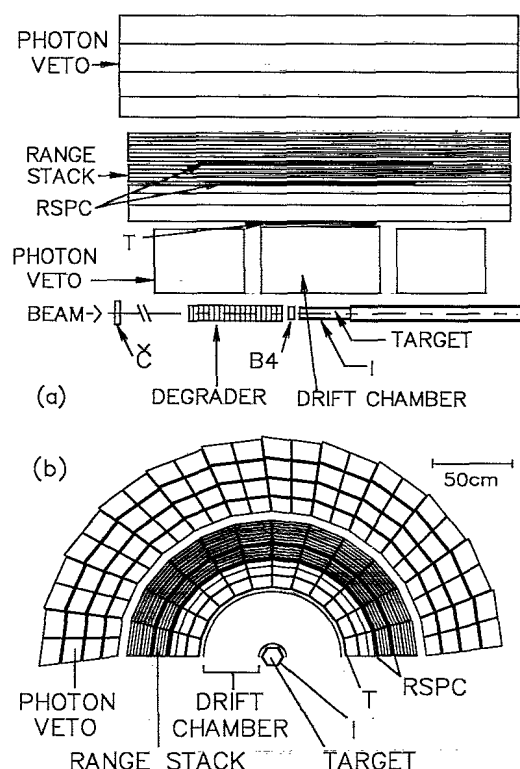


FIG. 1. (a) Side and (b) end views of the upper half of the cylindrically symmetric E-787 spectrometer.  $I$  and  $T$  are trigger counters that restrict the solid angle for accepting charged tracks to  $2\pi$  sr. Each trapezoid in (b) represents a counter with a photomultiplier at each end.

tectors—the range stack, the  $B4$  beam counter, the  $I$  counters surrounding the target, and the target itself, including its light guides which are scintillator—allows their use for photon, as well as charged-particle, detection. In each event, the area and arrival time of pulses from each counter are recorded.

Because the photon detectors are used as a veto, what is important is the likelihood that fluctuations in a photon's visible energy (energy deposited in scintillator) will give an observed energy below threshold. Fluctuations are dominated by the sampling of electromagnetic showers in the lead-scintillator barrel and end caps, with an additional rare but important component due to photonuclear interactions. The Monte Carlo simulation program<sup>9</sup> EGS predicts that our geometry, including support structures, will result in an average visible energy fraction of 0.29 in these detectors with very little energy dependence over the range of interest. This prediction is confirmed by the solid histogram in Fig. 2 which shows the total energy (corrected for the predicted visible energy fraction) in the barrel, end caps, and range stack, excluding that associated with a charged track, for events tagged as having a 205-MeV/c  $\pi^0$  ( $E_{\pi^0} = 245.5$  MeV, indicated by the vertical dashed line). Also confirmed is the calibration of the visible energy scale in each

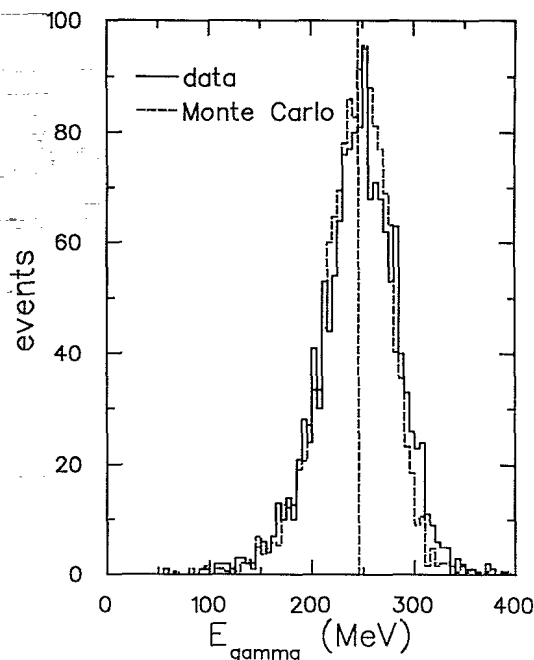


FIG. 2. Total photon energy (visible energy corrected for visible energy fraction) for events identified as  $K^+ \rightarrow \pi^+ \pi^0$  using only the  $\pi^+$ . The  $\pi^0$ 's energy in such events is indicated by the vertical dashed line.

counter, accomplished using cosmic-ray muons in the barrel and muons from  $K^+ \rightarrow \mu^+ \nu$  decays in the other detectors. The dashed histogram in Fig. 2 is the spectrum from a detailed Monte Carlo simulation of  $K^+ \rightarrow \pi^+ \pi^0$  decays in the spectrometer. It is calculated in the same way as the solid curve: Visible energy depositions are corrected for the visible energy fraction and summed. The agreement of these spectra demonstrates our understanding of both the physics of the energy deposition and the detailed geometry of the detectors.

The two-step process  $K^+ \rightarrow \pi^+ \pi^0, \pi^0 \rightarrow \nu \bar{\nu}$  would appear among  $K^+ \rightarrow \pi^+ \nu \bar{\nu}$  candidate events at a  $\pi^+$  momentum of 205 MeV/c. Our  $K^+ \rightarrow \pi^+ \nu \bar{\nu}$  analysis<sup>5</sup> is performed above this region to avoid  $K^+ \rightarrow \pi^+ \pi^0$  decays in which our photon detectors fail to find energy from the  $\pi^0$ . Prior to this restriction, made as the last step in the analysis, the only requirements in the  $K^+ \rightarrow \pi^+ \nu \bar{\nu}$  search specifically biased against  $K^+ \rightarrow \pi^+ \pi^0, \pi^0 \rightarrow \nu \bar{\nu}$  events are the kinematic cuts implicit in the trigger, the most restrictive of which is a minimum range requirement for the  $\pi^+$ . As over half of the  $K^+ \rightarrow \pi^+ \pi^0$  events in our charged-track solid angle meet this requirement, we use as a data sample for the  $\pi^0 \rightarrow \nu \bar{\nu}$  limit events surviving the  $K^+ \rightarrow \pi^+ \nu \bar{\nu}$  trigger and analysis prior to the final kinematic cuts.

This sample starts with  $2.0 \times 10^6$  triggers recorded in an exposure of  $1.05 \times 10^{10}$  stopped kaons. The  $K^+ \rightarrow \pi^+ \nu \bar{\nu}$  analysis<sup>10</sup> includes a veto on signals from a pion-sensitive Cherenkov counter in the beam and requires a 2-ns delay between the beam  $K^+$  and the decay

$\pi^+$  to ensure that the events are from a  $K^+$  that stopped in the target. It requires the unambiguous reconstruction of a single charged decay track in the target, drift chamber, and range stack, and identification of the track as a  $\pi^+$ .

For the  $\pi^0 \rightarrow \nu\bar{\nu}$  study, we use tighter photon cuts than are needed for the  $K^+ \rightarrow \pi^+\nu\bar{\nu}$  search. We apply separate cuts in the target and the rest of the detector. In the target, hits not associated with the  $K^+$  or  $\pi^+$  tracks are counted as photon energy if they occurred within 6 ns of  $t_{dk}$ , the time of the  $K^+$  decay defined by range-stack signals from the  $\pi^+$ . (All counters are calibrated so that signals of outward-propagating particles from a single event appear at  $t_{dk}$ .) Two or more target hits summing to greater than 2 MeV, or a single hit of greater than 5 MeV, veto the event. Individual visible energy depositions in the rest of the detector (range stack, barrel veto, end caps, and  $I$  counters) are initially categorized as prompt if they occur within 8 ns of  $t_{dk}$ . The time spectrum of visible energy depositions in the range stack and barrel shows a late tail, extending to over 20 ns. The time window defining prompt energy is thus extended to 24 ns after  $t_{dk}$  in these detectors. The sum of all prompt visible energy, excluding the target and the  $\pi^+$  in the range stack, is required to be less than 0.6 MeV. Events with a photon obscured by the  $\pi^+$  are removed by requiring that the observed energy in the inner-range-stack layers struck by the charged track does not greatly exceed that expected from the  $\pi^+$  alone. Figure 3(a) shows the survivors of this analysis, plotted against the range (in cm of scintillator) of the  $\pi^+$ . The figure contains 58 events, 27 in a clear  $K^+ \rightarrow \pi^+\pi^0$  peak with range less than 35 cm, and the remaining 31 concentrated in the region where misidentified  $K^+ \rightarrow \mu^+\nu$  events are expected.

The acceptance for  $K^+ \rightarrow \pi^+\pi^0, \pi^0 \rightarrow \nu\bar{\nu}$  is determined directly from  $K^+ \rightarrow \pi^+\pi^0$  events recorded as monitors along with the  $K^+ \rightarrow \pi^+\nu\bar{\nu}$  sample. All the trigger and analysis requirements except explicit photon cuts are applied. The range spectrum of events surviving this analysis is shown in Fig. 3(b). The acceptance for  $K^+ \rightarrow \pi^+\pi^0$  is

$$A_0 = \frac{N(\pi^+\pi^0)}{K(\pi^+\pi^0)B(\pi^+\pi^0)} \\ = \frac{805}{93267 \times 0.2117} = 0.041 \pm 0.001,$$

where  $N(\pi^+\pi^0)$  is the number of surviving events with range less than 35 cm,  $K(\pi^+\pi^0)$  is the number of stopping kaons for this sample,  $B(\pi^+\pi^0)$  is the known branching ratio<sup>11</sup> for  $K^+ \rightarrow \pi^+\pi^0$ , and the error shown is statistical. The acceptance  $A$  for  $K^+ \rightarrow \pi^+\pi^0, \pi^0 \rightarrow \nu\bar{\nu}$  is derived from  $A_0$  by including two effects due to photons. The first is random energy depositions that cause the photon cuts to occasionally reject photonless events, lowering the acceptance. The losses are mea-

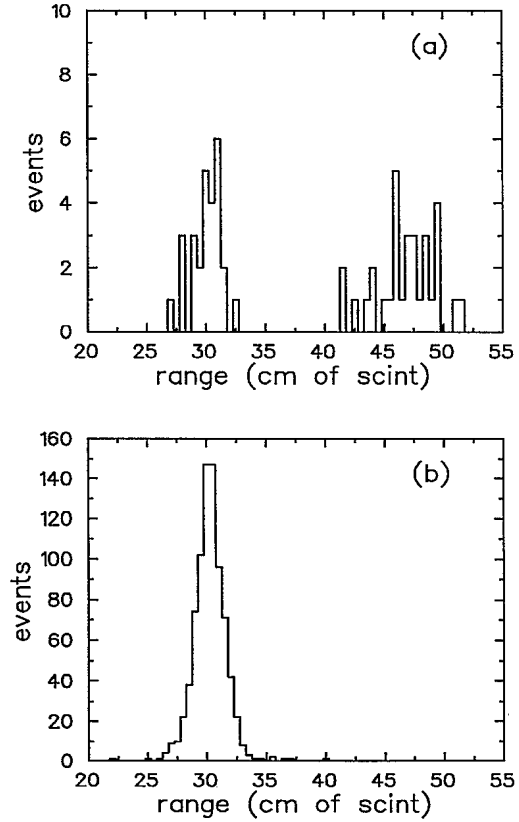


FIG. 3. Range spectrum for (a) events surviving the  $K^+ \rightarrow \pi^+\nu\bar{\nu}$  analysis and tight photon-rejection cuts, and (b)  $K^+ \rightarrow \pi^+\pi^0$  triggers surviving all charged-track cuts.

sured by applying the photon cuts to a sample of  $K^+ \rightarrow \mu^+\nu$  events,<sup>12</sup> resulting in an accidental-loss correction of  $C_{acc} = 0.39 \pm 0.01$ . The second effect is due to the fact that the  $K^+ \rightarrow \pi^+\pi^0$  events used to determine  $A_0$  do have photons in them. These photons can disrupt the charged-track analysis, lowering the acceptance in ways that would not occur to events with  $\pi^0 \rightarrow \nu\bar{\nu}$ . The disruptive effect of the photons on each trigger and analysis requirement not explicitly intended to reject photons is determined by comparing efficiencies for  $K^+ \rightarrow \pi^+\pi^0$  and  $K^+ \rightarrow \mu^+\nu$  monitor data and by comparing Monte Carlo simulations of  $K^+ \rightarrow \pi^+\pi^0$  events with and without the photons from the  $\pi^0$  decay. The resulting correction is  $C_{dis} = 1.19 \pm 0.02$ . Our overall acceptance, with statistical errors, for photonless  $K^+ \rightarrow \pi^+\pi^0$  decays is thus  $A = A_0 C_{acc} C_{dis} = 0.019 \pm 0.001$ .

With this acceptance, the flux of stopped kaons, and the known  $K^+ \rightarrow \pi^+\pi^0$  branching ratio, the 27 surviving events correspond to a branching ratio for  $K^+ \rightarrow \pi^+\pi^0$  with no observed photons of  $6.3 \times 10^{-7}$ . This rate is consistent with the rate of such events that we expect from the photon-detection inefficiency of the spectrometer, based on Monte Carlo estimates. The calculated fraction of missed  $\pi^0 \rightarrow \gamma\gamma$  events is  $(1.2 \pm 0.3) \times 10^{-6}$  with statistical errors. Systematic uncertainties are larger, perhaps as much as an order of magnitude in the es-

timated rate. The photon spectrum from  $\pi^0$ 's in  $K^+ \rightarrow \pi^+\pi^0$  at rest is flat from 20 to 225 MeV, with the sum of the two photon energies being 245.5 MeV. The Monte Carlo study indicates that the dominant mechanism for missing a  $\pi^0$  is the coincidence of (1) loss of the lower-energy photon due to sampling fluctuations and (2) loss of the higher-energy photon due to a photonuclear interaction in which the reaction products are not detected. This calculation qualitatively reproduces the tail of late energy depositions; these are due to remote interactions of slow neutrons from otherwise undetected photonuclear interactions. The systematic effects in the  $\pi^0 \rightarrow \gamma\gamma$  detection inefficiency are dominated by uncertainties in how a nucleus will deexcite after a photonuclear interaction and by how much energy will be detected.

Since we have a conventional explanation of the 27 events surviving the analysis, but our calculations are too uncertain to allow a sensible background subtraction, we use the measured rate to give an upper limit on the branching ratio for  $\pi^0 \rightarrow \nu\bar{\nu}$ :

$$B(\pi^0 \rightarrow \nu\bar{\nu}) < \frac{N_{90}(\bar{\gamma})}{K(\bar{\gamma})B(\pi^+\pi^0)A} = \frac{N_{90}(\bar{\gamma})}{K(\bar{\gamma})} \frac{K(\pi^+\pi^0)}{N(\pi^+\pi^0)} \frac{1}{C_{\text{acc}}C_{\text{dis}}},$$

where  $\bar{\gamma}$  and  $\pi^+\pi^0$  refer to the analyses with and without photon cuts, the latter being the raw acceptance calculation,  $K$  and  $N$  are the numbers of stopping kaons and surviving events in each analysis, and Poisson statistics is used to turn the observed 27 events into the 90%-C.L.  $N_{90}(\bar{\gamma})$ . Presenting the result in the latter form emphasizes the cancellation of systematic effects, notably the determination of the fraction of the kaon flux that decays at rest in the target. It should also be noted that Monte Carlo calculation enters only as part of the correction factor  $C_{\text{dis}}$ . Our resulting upper limit is

$$B(\pi^0 \rightarrow \nu\bar{\nu}) < \frac{35}{1.05 \times 10^{10}} \frac{93\,267}{805} \frac{1}{1.19 \times 0.39} = 8.3 \times 10^{-7} \quad (90\% \text{ C.L.}).$$

This is a factor-of-10 improvement over the beam-dump limit and a factor-of-30 improvement over the old direct limit.

This research was supported in part by the U.S. Department of Energy under Contracts No. DE-AC02-76CH00016, No. W-7405-ENG-36, and No. DE-AC02-76ER03072, and by the Natural Sciences and Engineering Research Council and the National Research Council of Canada.

(a)Current address: Joseph Henry Laboratories, Princeton University, Princeton, NJ 08544.

(b)Current address: Cornell University, Ithaca, NY 14853.

(c)Current address: Université de Montréal, Québec, Canada H3C 3J7.

<sup>1</sup>M. A. Bég, W. J. Marciano, and M. Ruderman, Phys. Rev. D **17**, 1395 (1978).

<sup>2</sup>H. Albrecht *et al.*, Phys. Lett. B **202**, 149 (1988).

<sup>3</sup>P. Herczeg and C. Hoffman, Phys. Lett. **100B**, 347 (1981).

<sup>4</sup>M. I. Dobrolyubov, A. Yu. Ignat'ev, and V. A. Matveev, Yad. Fiz. **47**, 468 (1988) [Sov. J. Nucl. Phys. **47**, 296 (1988)].

<sup>5</sup>M. S. Atiya *et al.*, Phys. Rev. Lett. **64**, 21 (1990).

<sup>6</sup>J. H. Klems, R. H. Hildebrand, and R. Stiening, Phys. Rev. D **4**, 66 (1971); G. D. Cable, R. H. Hildebrand, C. Y. Pang, and R. Stiening, Phys. Rev. D **8**, 3807 (1973).

<sup>7</sup>C. Hoffman, Phys. Lett. B **208**, 149 (1988).

<sup>8</sup>A. A. Natale, Instituto de Física Teórica, São Paulo, Report No. IFT/P-21/90 (unpublished); E. Fischbach *et al.*, Phys. Rev. D **13**, 1523 (1976).

<sup>9</sup>R. Ford and W. Nelson, Stanford Linear Accelerator Center Report No. SLAC-210, 1978 (unpublished).

<sup>10</sup>The sample used here was generated by a preliminary version of the analysis described in Ref. 5. The final version contained stricter particle-identification requirements that eliminated the remaining  $K^+ \rightarrow \mu^+\nu$  events. Retaining some of these events here provides a useful measure of the acceptance of the tighter photon cuts used in the  $\pi^0 \rightarrow \nu\bar{\nu}$  study.

<sup>11</sup>Particle Data Group, J. J. Hernández *et al.*, Phys. Lett. B **239**, II-8 (1990).

<sup>12</sup>The acceptance calculation for the cut on photon energy overlapping the  $\pi^+$  track uses  $K^+ \rightarrow \pi^+\pi^0$  events with both photons observed.